JOURNAL OF PROPULSION AND POWER
Vol. 16, No. 3, May–June 2000

Ultrasonic Method Applied to Full-Scale Solid Rocket Motors

Franck Cauty*
ONERA, F92322 Châtillon CEDEX, France

The solid rocket design engineer requires a multitude of data during the static and flight test phases of a development program. For instance, a better knowledge of the behavior of the internal thermal insulator, especially in the flap zones, is useful for determining the margins of safety. This, in addition to the heavy work on the modelization of the insulation degradation, is why a measurement tool for determining the behavior of the insulators has been developed. This technique is direct, nonintrusive, and based on the propagation of ultrasonic waves through the materials: case, insulator, solid propellant, etc. By following the evolution of the echoes coming back from the regression surface or the degraded zone of the insulator in real time, many times per second during the test, one can deduce the following data: the sequence of events at the measurement location, the starting time of degradation and ablation of the insulator, and, coupled with thermoablative computing code, the pyrolysis rate and the heat flux evolution received on the insulator surface. For solid propellant, the displacement of its combustion front along the insulator is followed, and of course its burning rate is deduced.

Nomenclature

C = mechanical wave velocity, m/s
dP/dt = pressure gradient, MPa/s
k_P = wave velocity variation coefficient with respect to pressure, MPa^{-1}
k_T = wave velocity variation coefficient with respect to temperature, K^{-1}
P = pressure, MPa
r_b, R_b = burning rate, mm/s
T = temperature, K
W = thickness, m
τ = propagation time, μs

Subscripts

P = pressure
ref = reference conditions
T = temperature

Introduction

ON full-scale solid rocket motors, the behavior of the internal thermal insulator (ITI) and the evolution of the combustion surface of the solid propellant (SP) grain have to be determined during a test for verifying the predictions. In the last 20 years, engineers have developed experimental nonintrusive tools aimed at determining the regression rate of energetic materials.[1] These techniques are based on wave propagation (x rays and ultrasound) or on material property variation (capacitance method).

Real-time radiography has been used successfully at Arnold Engineering Development Center,[2,3] Société Nationale des Poudres et Explosifs (SNPE),[4,5] and China Lake[6] to image a variety of events in solid rocket-motor firings: insulator erosion, combustion surface evolution, propellant burning rate, slag accumulation, and others. The images produced by x-ray systems must be interpreted to determine the material surface position. Image processing has become a powerful tool in analyzing radiography: mapping techniques, noise removal, image segmentation, grayscale morphology, frame-by-frame processing, and digitization.

Received 29 November 1998; revision received 15 April 1999; accepted for publication 15 May 1999.

*Research Engineer, BP 72, Energetics Department.

The plasma capacitance gauges (PCG) technique was developed in the United States during the 1980s at TRW[7] and in France at ONERA[8] in the 1990s mostly to measure internal insulator erosion. This technique is based on the variation of the electrical capacity with the time, which is related directly to the thickness of the material between the electrodes. The capacitance increases as the thickness of material decreases, and these data yield real-time information on insulation thickness and behavior and, possibly, on flame arrival time. This technique was applied to subscale and full-scale motors, fired on the ground as well as in flight.[7]

ONERA has been applying its well-known ultrasonic method for more than 20 years in SP combustion studies.[9–15] This measurement method stands as an industrial control procedure at SNPE, the French propellant manufacturer. We have adapted this tool for determining the behavior of the internal insulator in the flap zones of full-scale rocket motors in relation with Société Européenne de Propulsion (SEP). This paper presents a description of the ultrasonic method, its specific instrumentation, the acoustic propagation behavior, and examples of data obtained on solid rocket-motor ground tests for insulator behavior as well as for SP behavior.

Ultrasound Method

Principle of the Method

The method, like the sonar technique, is based on the propagation time measurement of an ultrasound wave through the tested material(s).[9,10,15] If the wave velocity C was constant, not modified by local conditions, the material thickness W would be only proportional to the propagation return time τ:

$$\tau = 2W/C \tag{1}$$

Unfortunately, wave propagation (velocity and damping) changes with the material temperature (initial value and thermal profile) and with the stress–strain distribution related to inner pressure:

$$C_{\text{ref}}/C = [1 + k_T(T - T_{\text{ref}})][1 - k_P(P - P_{\text{ref}})] \tag{2}$$

These effects will be stronger under unsteady conditions, that is, pressure or heat flux variations. There are different behaviors related to the regression rate level of the tested material. The limit on regression rate would be about 1 mm/s. Above this value, which corresponds to most SP regression rates, the thermal profile has no significant effect on the web distance burned and on the burning rate, but the pressure-induced stress effect (called pressure effect) has to be taken into account to correct the burning rate values due to pressure-gradient dP/dt sensitivity of the ultrasonic measurement.[10]

For low-rate degradation or combustion phenomena, the pressure effect does not have to be canceled out. The main parameter becomes the thermal profile variation. The ultrasonic echo time location will be modified by the quantity of heat within the material. When the temperature is increasing, the wave velocity decreases and the echo time location rises. Examples will show that the heat flux has as much an effect as the degradation itself.

Ultrasonic Instrumentation

The behavior of the ITI such as silica-filled ethylene-propylene diene monomer (EPDM) requires a few extra instrumentation tools. The internal insulators used in solid rocket motors (SRM) are degraded by the heat flux coming from the combustion gases, partly by radiative transfer and partly by convective exchange (Fig. 1). This pyrolysis process is modified by the core flow velocity stripping off the char residue from its surface and, in a flight condition, also is modified due to acceleration, vibrations, and particle impact. Once the char is ejected, ablation occurs, and the regression rate of the insulator surface is increased by a significant factor. The ultrasonic wave is reflected somewhere in the pyrolysis zone (porosity limit) so that the ejection of the residue is only seen via the heat flux variation induced.

Inasmuch as the echoes' characteristics are markedly modified by the heat flux variations, a new ultrasonic measuring system has been developed. The ultrasonic signal itself has to be digitized for postprocessing rather than being processed in real time.

The ultrasound equipment is composed of 10 ultrasonic emitter–receiver devices triggered by a 1-kHz internal clock (Fig. 2). One selects the channel number required for the test and adapts the final repetition rate for the multiplexed ultrasonic signals for personal computer data acquisition. This repetition rate should be less than 500 Hz due to personal computer storage speed limitations. Special software has been developed by Sofratest Company. The ultrasonic signal is selected and digitized in a time window following the emission pulse by a high-speed (10-, 25-, or 50-MHz) A/D converter. The window time range and an initial time delay for masking the emission damping tie or nonsuitable echoes are selected. Echoes are stored for postrun analysis.

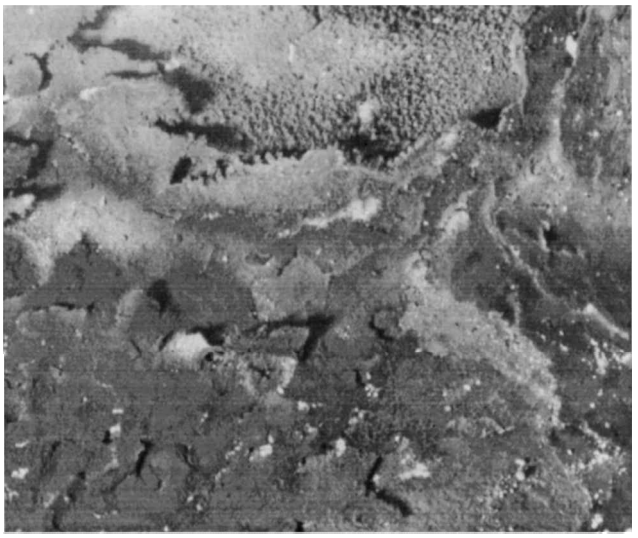

Fig. 1 Silica-filled EPDM char residue.

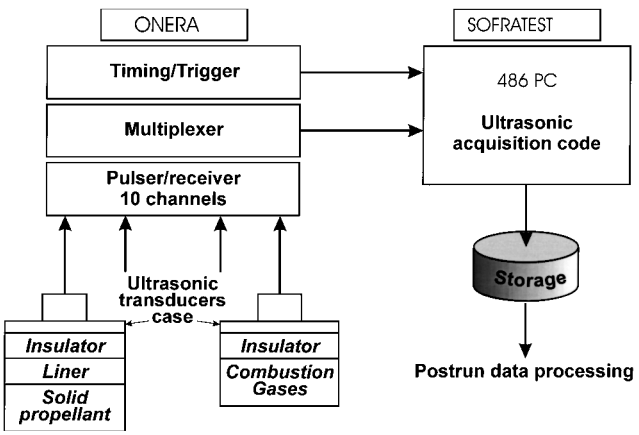

Fig. 2 Layout of the ultrasound measurement system.

Postrun Ultrasound Analysis

Specific data processing techniques have been developed for stored ultrasonic echoes analysis. The echoes corresponding to the material surface of interest are shown in Fig. 3. These pulse trains are composed of a few positive and negative peaks. [Note that in all of the figures representing ultrasound echoes, similar to an oscilloscope image, the ordinate is unlabeled. It corresponds to an arbitrary voltage. The x coordinate is always a propagation time (τ in microseconds.)] The propagation time variation is usually obtained from the displacement of the zero crossing time of the major negative or positive echo peak. This point is the least sensitive to amplitude variation.[15] While processing ITI digitized ultrasound echoes, experience shows that this particular point is difficult to follow throughout the test. In fact, this leads to a survey of a few measurement points in the pulse train: points of major amplitude (positive and negative parts), selected amplitude points (threshold level), and of course the zero crossing points. The evolution of these points is determined as a function of time; thus, one can choose those that give a continuous representation of the pulse behavior. This is the first step in data processing.

Sometimes the results are disappointing. The ultrasonic echo amplitude is too small compared to background and baseline echoes due to the poor quality of the acoustic propagation or to a drastic drop of the amplitude during the test itself (Fig. 4). Furthermore, selected and baseline echoes can be mixed, and a misunderstanding of the propagation time variation occurs. Because of this, correlation techniques are utilized based on several digitized ultrasound windows. This results in an ultrasound trace without echoes other than those coming from the reflection surface displacement (Fig. 5). From these processed ultrasonic windows, specific points are selected, and the propagation time variation is obtained. The evolution of the major amplitude level of the return echoes is also computed as in the first level of analysis because it can be helpful in understanding the ultrasound echoes' behavior. A few measurement examples

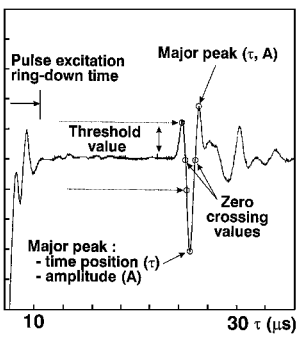

Fig. 3 Typical ultrasound echoes and detection specific points.

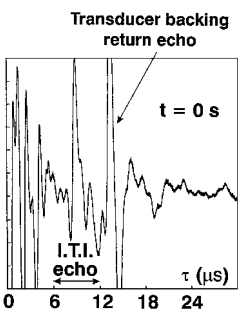

Fig. 4 Mixing of echoes from the insulator with the baseline (rough data).

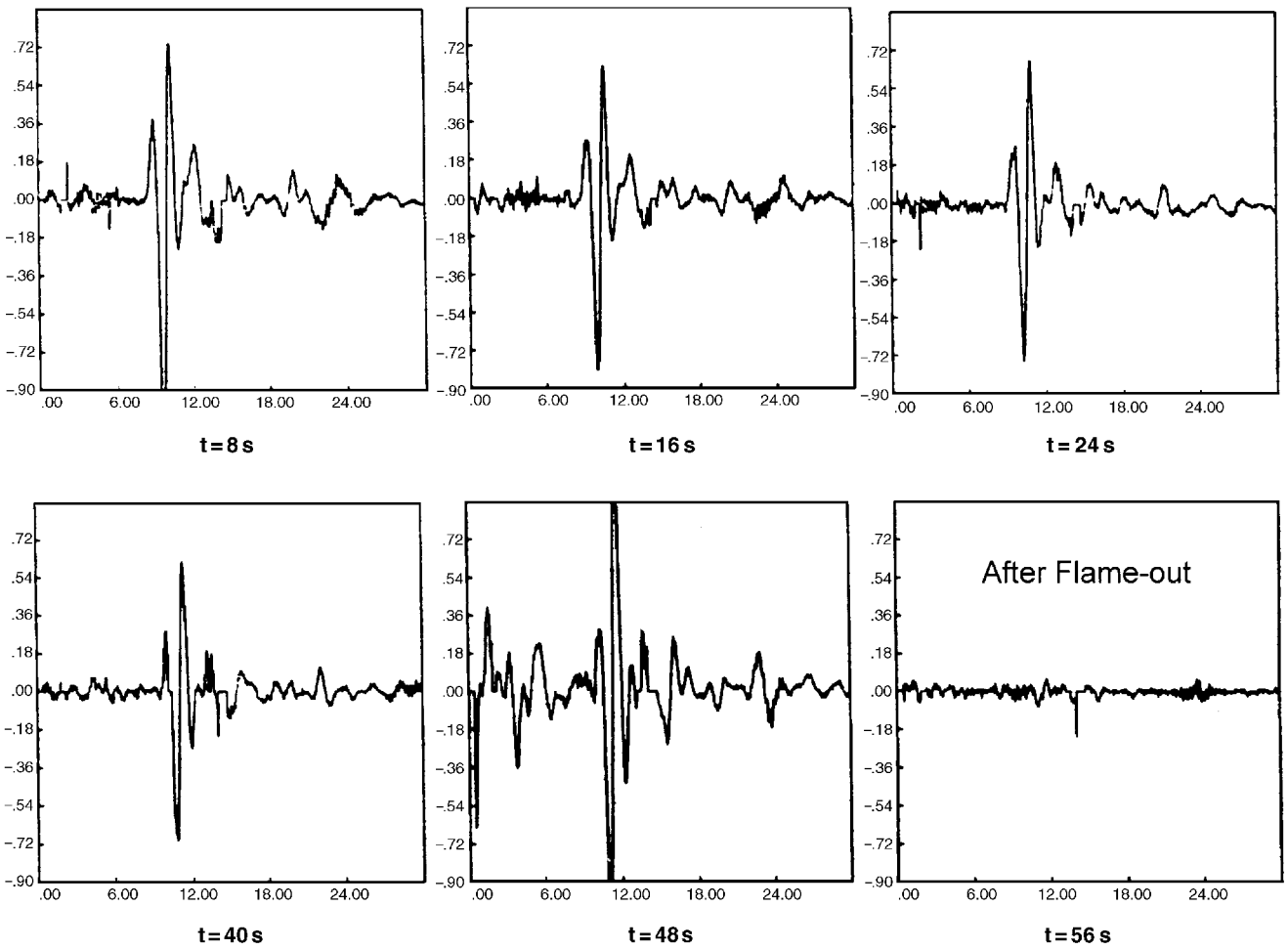

Fig. 5 Echoes evolution after postrun correlation processing.

will illustrate the ability of the data processing in catching echoes evolution.

Experimental Results

The ultrasonic measurement method is applied to large-scale solid rocket motors fired in static test facilities in France as well as in the United States.[16] Two kinds of results are presented: the internal insulator degradation process and SP combustion.

ITI

As a contribution to a better prediction of the required thickness of an insulator, data from the degradation process are studied in the flap zones. In these zones, the degraded thickness is usually small but depends on the location along the case.

The first example shows the influence of the SP grain weight on the insulator degradation during a static test. The SRM was fired horizontally. The flap zone is opened in the upper part of the motor and closed in the lower part. Heat flux level and time sequence differ considerably between the upper and lower parts at the head end of the motor where the measurements were performed (Fig. 6). At the beginning of the burning, ultrasound echoes variations correspond to an increase in the propagation time due to heat effect on the speed of sound. In other words, it works like a fluxmeter. The propagation time evolution varies as the burning surface of the propellant grain reaches the transducer location. Following the predicted burning surface evolution, the heat flux received by the insulator rises and modifies the slope of the propagation time variation. Next, the balance between thermal effect and pyrolysis surface regression changes with the insulation degradation. This occurs around 8 s after the ignition on the upper side and is delayed up to 22 s on the lower side because of the protective effect of the closed flap.

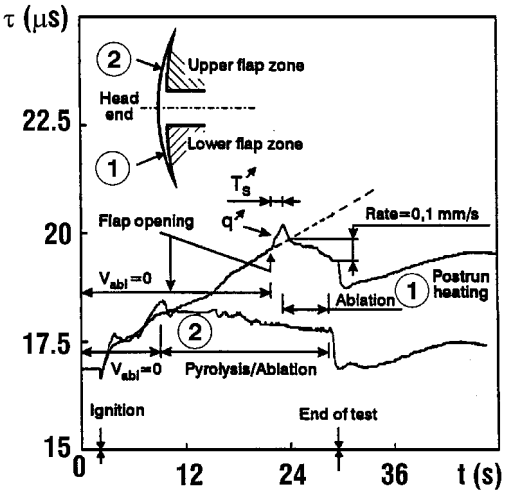

Fig. 6 Propagation time variation at two head-end flap zone locations: behavior of the internal insulation.

Just before the propagation time reduction with the pyrolysis, there is a peak corresponding to the surface temperature climb from a preheated value to a level over the pyrolysis threshold limit.

A mean value of the pyrolysis rate is deduced from propagation time variation, but an understanding of insulation behavior is not complete without a comparison with theoretical behavior determined from a thermo-erosive (or -ablative) code PTIMAD developed by SEP and ONERA. There is no direct relationship between propagation time variation and degraded thickness. The wave velocity varies depending on the temperature; thus, the thermal

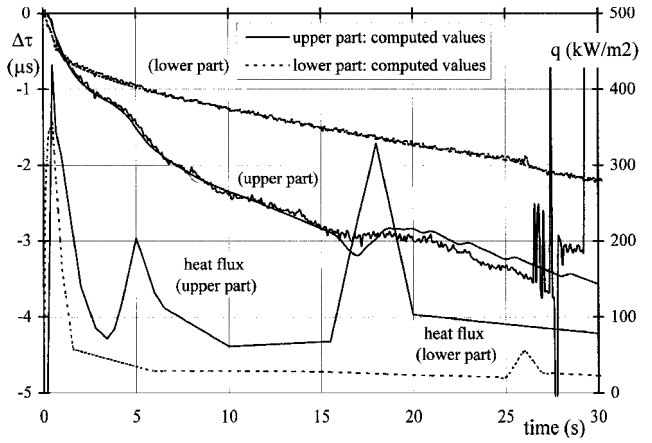

Fig. 7 Heat flux sequence determined from computed/measured propagation time variation.

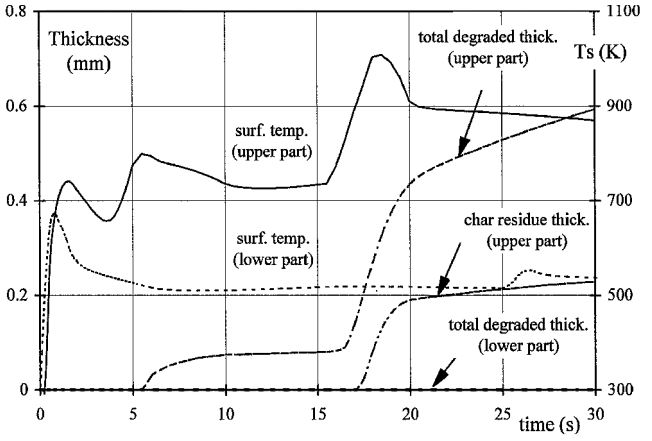

Fig. 8 Computed surface temperature and degraded thickness.

profile has to be known to determine, at any time, the degraded thickness (if any) of the ITI. Criteria are established for the propagation of sound through the pyrolysis zone: its acoustic wave velocity as a function of the temperature (700–1000 K) and its reflection limit with respect to porosity or minimum density value. These characteristics are too difficult to be measured, and so they are fitted from the ultrasonic measurement data already obtained.

The measured propagation time is compared to a calculated one deduced from a heat flux history, input data of the PTIMAD thermoerosive code. This work was also done for a second horizontally fired SRM (static test). The propagation time variations obtained at the two head-end isoradius locations are shown in Fig. 7. The internal pressure effect is removed and measured, and calculated evolutions are compared. Finally, evolutions are defined in terms of the order of magnitude of the received heat flux, the surface temperature, and the degraded zone and char thickness (Fig. 8), which are very useful to the engineer in charge of insulation sizing.

The ultrasound measurement at the lower part shows a small level of heat flux, which is slightly decreasing (level below 50 kW/m^2) after an initial peak that corresponds to the combustion gases filling the flap gap. On the upper part of the head end insulator, the deduced heat flux highlights two peaks: 200 kW/m^2 at 5 s and 320 kW/m^2 at 18 s. The baseline flux is twice the level at this location. At the lower part, the surface temperature never goes over 700 K, which should be considered as the low-limit temperature for degradation. The temperature is kept nearly constant at around 500 K, up to $t = 30$ s. For the other location, the temperature is increased at each heat peak: from 700 to 780 K and then from 730 to 1000 K. After the first temperature climb, the insulator degradation process starts at a first step of less than 0.1 mm, then this process increases drastically with the second peak. Notice a slope variation on the propagation time variation due to the strong degradation.

The total degraded thickness obtained from the measurement and the computations have to be compared to pre/post test control. Up to now, these results have been accurate enough to confirm interest in the ultrasound method.

SP Combustion

The ultrasonic method is applied to SP burning measurement in solid rocket motors. This is aimed at surveying the grain combustion along the liner (timer function) and at determining the web distance burned and the burning rate at the end of the grain combustion.

The grain combustion evolution is sought by using at least two or three ultrasonic transducers bonded closely to each other at a distance of a few centimeters along an axial line. As long as the SP exists, no significant echo is seen at the interface between the liner and the SP. When the combustion profile is passing by the transducer location, echoes appear, corresponding to the surface of the liner becoming free (Fig. 9). Then, its heating and its degradation could be measured. The timer function requires echo processings. In Fig. 10, a typical sequence of echoes represents how the acoustic field is modified by the lateral displacement of the burning front. The criterion for the lateral combustion appearance time stands as the first ultrasonic window on which an echo appears. Once the passing-by times at several locations are known, one can deduce the surface burning rate of the propellant. If the normal burning rate is determined at the same time on the grain, obviously an overrate level is obtained (if any).

In fact, measuring the propagation time through the propellant grain and computing its burning rate during the test for such large rocket motors is not easy. Basically, this is a question of acoustic energy, thus of transducer size and of frequency. The SPs have a heavy damping coefficient for mechanical waves due to scattering.[17]

The conditions for data acquisition were focused on the thermal insulator behavior: short-time duration of the ultrasonic digitized window (30–50 μs), internal insulation echoes centered through the window, and 10 ultrasonic transducers operating, so that a low repetition rate per channel (25–40 Hz) is achieved (Fig. 11). This is why the echoes obtained from the SP burning surface are coming from only a few centimeters inside the grain up to zero thickness.

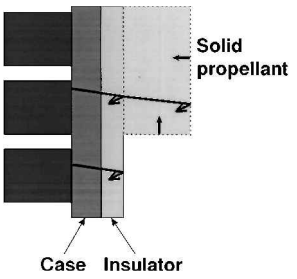

Fig. 9 Transducer implementation for timer function.

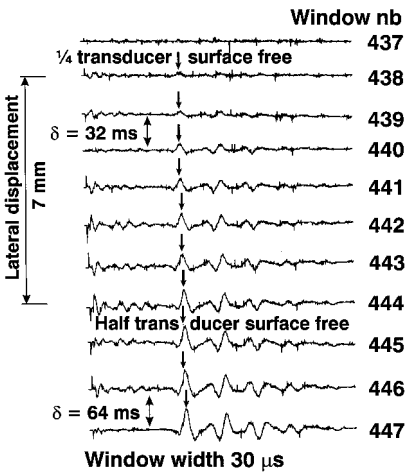

Fig. 10 Time sequence of the lateral displacement of the burning surface.

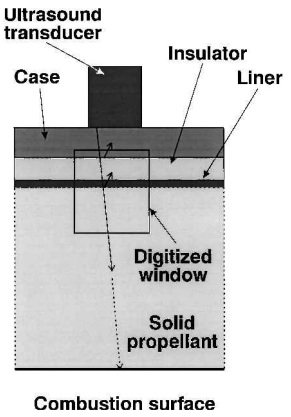

Fig. 11 Ultrasound operating conditions.

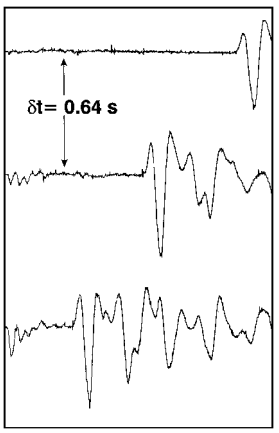

Fig. 12 Solid propellant end burning time sequence.

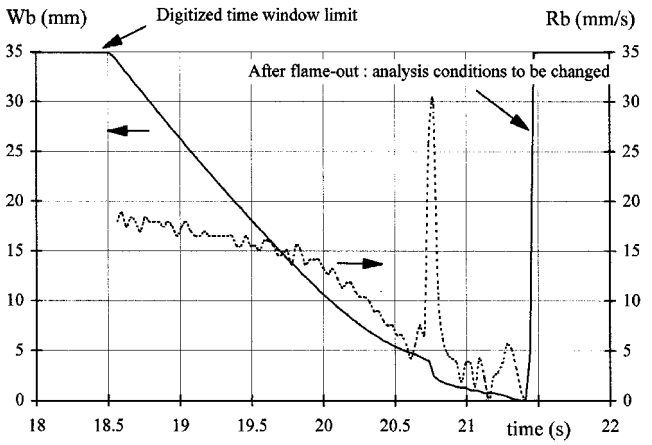

Fig. 13 Web distance burned and burning rate at the end burning of the grain.

The displacement of the burning surface echoes on the ultrasonic digitized window is quicker: The echoes shown in Fig. 12 represent their shifting for a time interval of 0.64 s (20 windows). The burning rate evolution (Fig. 13) deduced via a mean wave velocity (more or less theoretical) for the tested propellant is accurate in comparison with the standard burning rate law that has been determined, for example, from the ultrasonic method in a small setup. Reduced scattering and fairly good evolution have to be pointed out in spite of, or because of, the small number of data points. On the web distance burned, as shown in Fig. 13, there is a drastic variation of burning rate in the thickness range 4–2 mm. It was not determined if the sign of the superficial overrate was due to the propellant cast or a measurement artifact. After the end of the propellant grain burning at the transducer location, the processing parameters have to be modified to follow the insulator behavior. Using the burning rate conditions, it goes out of range once the zero thickness is obtained.

This analysis does not take into account the angle that can exist between the burning surface and a plan parallel to the ultrasonic transducer, but this cosine value is close to unity because a few degrees of slope tend to make the waves in the transducer disappear (optical path–emission/reception transducer).

Conclusions

The ultrasonic measurement method described gives data about material insulation degradation behavior and about SP burning. Values of thermal insulator degradation thickness and rate, surface temperature, and heat flux evolution are obtained for any burning time, coupled with a suitable thermo-ablative computer code. This method does not only lead to thickness determination but, also, the analysis leads to entire time sequence and heat flux history. This is much more than classical before/after test control. This is a nondestructive testing method. That means the case, the insulator, the liner, the SP, and their bondings are controlled at any given time during the firing. Thus, internal damage dewetting can be highlighted if a transducer is located at the default area.

Comparison with other techniques, such as PCG, another promising method, is welcome. These two methods are of mutual interest because they complement each other. For internal insulators, PCG seeks the external surface of the char residue and the gas boundary layer (external/gas-phase part). The ultrasound method follows the pyrolysis front through the material (solid-phase part).

Up until the present time, this work has been focused on improving the quality of the analysis by multiplying the static test measurements. In the flap zones, a map of the insulation behavior could be drawn easily; a better understanding could come from a correlation with the flap-gap distance measured by eddy current sensors.

For SP applications, the needs exist for the detection of the flame passing by at a specific location, for the burning rate level along the liner, for checking of burning rate level depending on the axial line (several batches/grain), for determining the web distance burned, and for the burning rate to be determined as deeply as possible (hump effect), which is required by the propellant manufacturer up to the grain central core. Efforts have to be focused on these aspects, especially in terms of ultrasonic transducers and associated apparatus.

The ultrasonic measurement method should flourish in the next few years. It has considerable promise and is able to be investigated as a new flight instrumentation.

Acknowledgments

The author would like to thank the Délégation Générale à l'Armement and the Société Européenne de Propulsion for the funding and the fruitful collaboration with us. Thanks to J. C. Démarais, C. Éradès, J. C. Godon, and C. Caugant (ONERA) for their highly appreciated work on this topic. The author also wishes to thank Centre d'Achèvement et d'Essais des Propulseurs et Engins for their help during the static test phases.

References

[1] Allen, W., "Assessment of Future Solid Rocket Motor Flight Instrumentation/Data Needs," *Journal of Spacecraft and Rockets*, Vol. 20, No. 2, 1983, pp. 164–171.

[2] "AEDC Test Highlights," Office of Public Affairs, Arnold Engineering Development Center, U.S. Air Force, Arnold AFB, TN, Fall 1992.

[3] Anderson, M. G., "Real-Time Radiography Support for Titan LAM," AIAA Paper 92-3823, July 1992.

[4] Tauzia, J. M., and Lamarque, P., "Solid Rocket Propellant Behavior During Static Firing Test Using Real Time X Ray Radiography," CP-598, AGARD, May 1998, pp. 35/1–6.

[5] Thépenier, J., "Solid Rocket Motor Behaviour During Static Firing Test Using Real Time X-Ray Radioscopy," *AIAA Solid Rocket Technical Committee Lecture Series, 36th Aerospace Sciences Meeting and Exhibit*, 1998.

[6] Rogerson, D., "Dynamic Real-Time Radioscopy," Solid Rocket Motor Test and Test Techniques, *AIAA Solid Rocket Technical Committee Lecture Series, 36th Aerospace Sciences Meeting and Exhibit*, 1998.

[7] Yang, L. C., Miner, E. L., and Romanos, T. C., "Application of Plasma Capacitance Gage (PCG) for Real Time Measurements of Solid Rocket Motor Internal Insulation Erosion," AIAA Paper 90-2327, July 1990.

[8]Seret, J., Démarais, J. C., Cauty, F., and Dupont, M., "Application des Techniques de Mesure d'Épaisseur à la Détermination de la Vitesse de Régression d'une Protection Thermique," *Fonctionnement des Moteurs à Propergol Solide Segmentés pour Lanceurs Spaciaux*, Colloque CNES/ONERA, Paris, 1992, pp. 21/1–23.

[9]Kuentzmann, P., Démarais, J. C., and Cauty, F., "Mesure de la Vitesse de Combustion des Propergols Solides par Ultrasons," *La Recherche Aérospatiale*, No. 1, 1979, pp. 55–79.

[10]Traineau, J. C., and Kuentzmann, P., "Ultrasonic Measurements of Solid Propellant Burning Rates in Nozzleless Rocket Motors," *Journal of Propulsion and Power*, Vol. 2, No. 3, 1986, pp. 215–222.

[11]Cauty, F., and Traineau, J. C., "Mesure par Ultrasons de la Vitesse de Combustion d'un Propergol Solide: Perfectionnement et Applications à Divers Régimes de Fonctionnement," *Proceedings of the 19th International Congress of Institut Chemische Technologie*, Institut Chemische Technologie, Karlsruhe, Germany, 1988, pp. 54/1–13.

[12]Godon, J. C., Duterque, J. R., and Lengellé, G., "Solid Propellant Erosive Burning," *Journal of Propulsion and Power*, Vol. 8, No. 4, 1992, pp. 741–747.

[13]Cauty, F., Démarais, J. C., and Éradès, C., "Determination of Solid Propellant Burning Rate Sensitivity to the Initial Temperature by the Ultrasonic Method," *Non Intrusive Combustion Diagnostics*, edited by K. K. Kuo and T. P. Parr, Begell House, New York, 1994, pp. 642–653.

[14]Cauty, F., "Measurement of Solid Propellant Response Function at Low Frequency by Means of Ultrasonic Method," *Ecoulements Propulsifs dans les Systèmes de Transport Spatiaux*, Proceedings of Colloque CNES/ONERA/CNRS, Vol. 1, 1995, pp. 101–116.

[15]Cauty, F., "Mesure par Ultrasons de la Vitesse de Combustion des Propergols Solides," ONERA TR 5/3173 EY, July 1983.

[16]"Acoustic Measurements During Solid Rocket Motor Testing," Arnold Engineering Development Center, U.S. Air Force, Arnold AFB, TN, Jan. 1995.

[17]Dumont, C., "Etude de la Propagation d'Ondes dans un Propergol Solide," *Revue d'Acoustique*, No. 63, 1982, pp. 242–245.